(ACCEPTED BY THE ASTROPHYSICAL JOURNAL LETTERS)
Preprint typeset using LaTeX style emulateapj v. 11/10/09

KEPLER OBSERVATIONS OF RAPID OPTICAL VARIABILITY IN ACTIVE GALACTIC NUCLEI

R. F. MUSHOTZKY[1,2,5], R. EDELSON[1], W. H. BAUMGARTNER[2,3], P. GANDHI[4]

(Submitted 9 Sep 2011; Accepted 31 Oct 2011)

ABSTRACT

Over three quarters in 2010–2011, Kepler monitored optical emission from four active galactic nuclei (AGN) with ∼30 min sampling, > 90% duty cycle and $\lesssim 0.1\%$ repeatability. These data determined the AGN optical fluctuation power spectral density functions (PSDs) over a wide range in temporal frequency. Fits to these PSDs yielded power law slopes of −2.6 to −3.3, much steeper than typically seen in the X-rays. We find evidence that individual AGN exhibit intrinsically different PSD slopes. The steep PSD fits are a challenge to recent AGN variability models but seem consistent with first order MRI theoretical calculations of accretion disk fluctuations.

Subject headings: Accretion, accretion disks — Black hole physics — Galaxies: active — Galaxies: Seyfert

1. INTRODUCTION

The optical continuum from active galactic nuclei (AGN) is believed to be dominated by emission from an accretion disk surrounding a supermassive black hole and can be adequately modeled as radiation from a simple Shakura-Sunyaev disk (Edelson & Malkan 1986). Because this region is too small to image (except via gravitational lensing; Kochanek 2004), indirect methods must be used to probe its structure and physical conditions. One of the best probes is provided by the strong variability seen throughout the optical/ultraviolet/X-ray bands in most AGN. However, limitations with many ground-based optical observations have made it difficult to obtain accurate, densely and regularly sampled data sets covering the large range of timescales necessary to constrain disk physics and search for characteristic times which may be related to orbital, dynamic or other expected timescales. In particular, diurnal and weather related interruptions can severely degrade the ground based sampling pattern and atmospheric seeing introduces photometric errors that are much larger than the Kepler uncertainties and often are as large as or larger than the intrinsic short timescale optical source variability. However ground based data have sampled much longer timescales than are available in the present Kepler data sets.

The natural timescales for a disk—light-crossing (t_l), dynamical (t_{dyn}), and thermal (t_{th}) timescales—are set by the black hole mass and the accretion processes (Frank, King & Raine 2002). The order of magnitude estimates for these timescales are: $t_l = 2.6\ M_7\ R_{100}$ hours, $t_{dyn} = 10\ M_7\ {R_{100}}^{3/2}$ days, and $t_{th} = 0.46\ M7\ {R_{100}}^{3/2}\ {\alpha_{0.01}}^{-1}$ years, where M_7 is the black hole mass in units of $10^7\ M_\odot$, R_{100} is the emission distance in units of 100 times the Schwarzschild radius $2GM/c^2$, and $\alpha_{0.01}$ is the Shakura-Sunyaev viscosity parameter (Shakura & Sunyaev 1973) divided by 100. For assumed Eddington ratios of 0.01–0.1 and mass ranges of 10^6–$10^9\ M_\odot$ typical for AGN, these natural timescales range from hours to years. Previous data have been unable to constrain the optical time variability over this wide range for any individual AGN.

The Kepler mission (Borucki et al. 2010) provides a solution to these observational difficulties. Kepler has been observing a ∼115 square degree region of sky, monitoring ∼165,000 sources every 29.4 minutes with unprecedented stability ($\lesssim 0.1\%$ for a 15th magnitude source) and high duty cycle (> 90%) over a period of years. During Q6 (Quarter 6: UT 24 June–22 September 2010), Q7 (23 September–22 December 2010) and Q8 (22 December 2010–24 March 2011), the Kepler target list included at least four variable AGN from our guest observer program. This paper reports initial results of Q6–Q8 (and in one instance Q4) observations of these Kepler AGN, focusing on fluctuation power spectral density analysis. The source selection, data collection and reduction are given in Section 2, the time series analysis and results are reported in Section 3, implications are discussed in Section 4, and brief conclusions presented in Section 5.

2. DATA

2.1. *Source Selection*

Because it lies at low galactic latitudes not systematically covered by major extragalactic or AGN surveys the Kepler field (∼0.3% of the sky) currently contains only a few catalogued AGN[6]. Targets must be identified and windows chosen before Kepler data can be downloaded. Thus we have undertaken extensive efforts to identify AGN in the Kepler field. This started with a database search to find previously identified AGN. We then applied the method of Stocke et al. (1983) to the Rosat all sky survey (RASS; Voges et al. 1999) to select AGN candidates based on their X-ray to optical flux ratio. We also used the 2MASS all sky survey catalog (Strutskie et al. 2006) to identify AGN candidates based on infrared colors (Malkan 2004) and association with a RASS source.

Table 1 gives details of the Kepler AGN whose light curves are presented in this paper, a sample of four variable AGN that Kepler has been observing since Q6. Of these four, only Zw 229–15 ($z = 0.0275$, Falco et al. 1999, Proust 1990) had been identified as an AGN prior to the launch of Kepler. A recent reverberation mapping campaign found it had an Hβ lag

[1] Department of Astronomy, University of Maryland College Park, College Park, MD 20742
[2] NASA/Goddard Space Flight Center, Astrophysics Science Division, Greenbelt, MD 20771
[3] Joint Center for Astrophysics, University of Maryland Baltimore County, Baltimore, MD 21250
[4] Institute of Space and Astronomical Science, Japan Aerospace Exploration Agency, 3-1-1 Yoshinodai, chuo-ku, Sagamihara, Kanagawa 252-5210, Japan
[5] Corresponding author: richard@astro.umd.edu

[6] However, a portion of the Kepler field is covered by SDSS/SEGUE, http://www.sdss.org/segue/

Table 1
Kepler AGN Reference Information

Source Name	Kepler ID	RA(J2000)	Dec(J2000)	z	RASS
Zw 229−15	6932990	19 05 26.0	+42 27 40	0.028	0.450
KA 1925+50	12158940	19 25 02.2	+50 43 14	0.067	0.170
KA 1858+48	11178007	18 58 01.1	+48 50 23	0.079	0.210
KA 1904+37	2694185	19 04 58.7	+37 55 41	0.089	0.023

Note. — Columns 1 and 2 give the source name (KA refers to newly discovered Kepler AGN first reported in this paper) and Kepler ID number, columns 3 and 4 give the position, column 5 the redshift, and column 6 the Rosat all sky survey (RASS) count rate in counts s^{-1}.

of ∼4 days and estimated its black hole mass at $\sim 10^7$ $M_\odot$ (Barth et al. 2011). The other three AGN in Table 1 were all discovered as a result of the search described above. (The prefix "KA" is used to designate newly identified Kepler AGN.) Spectra of these three, plus ten other newly discovered Kepler AGN are given in Edelson & Malkan (2012).

2.2. *Kepler SAP Light Curves*

The Kepler standard data processing pipeline (Jenkins et al. 2010), operates on original spacecraft data to produce calibrated pixel data (Quintana et al. 2011). The next step, PA, uses simple aperture photometry to extract SAP_FLUX count rates from these 2-dimensional images (Twicken et al. 2011). The spacecraft downloads not full CCD frames but only "postage stamp" images for the targets. Only a fraction of the downloaded pixels are used in the extraction. The next step in the standard pipeline, SAPPDC, conditions the light curves for transit searches, outputting PDC_FLUX light curves. However, no conditioning occurred for sources presented in this paper (the SAP_FLUX and PDC_FLUX data are identical to within a constant offset), so this and all further steps are not relevant to the current work. We use SAP_FLUX count rates for our AGN light curve analyses. These light curves are presented in Figures 1 and 2.

Kepler, with its $\lesssim 0.1\%$ repeatability, $> 90\%$ duty cycle and durations of years, explores a level of data quality superior to anything previously obtained. Thus one must be concerned about other sources of error, especially systematic errors, in this relatively young mission. An independent check of the Kepler data is available for Zw229−15 since in 2010, it was observed by both Kepler and the ground based Lick AGN Monitoring Program (LAMP). These light curves, shown in Figure 1, indicate a very good agreement between Kepler and independent ground based LAMP data, well within the LAMP ∼1% errors and so, at least in this case, the systematic and other errors in the Zw 229−15 data are generally no larger than the ∼1% LAMP errors.

However, the quoted Kepler errors are much smaller, and there is currently no way to be sure that systematic errors are not affecting the data at the level between ∼0.1% and ∼1%. Indeed, Figure 2 shows that small, short term (1–2 day), discontinuities are sometimes observed following monthly data downloads or safe mode events. This is believed to arise from thermally induced focus changes as the solar illumination changes during spacecraft slews[7]. Both our group and the Kepler team are working to correct for this in future analyses. While our understanding will undoubtedly improve as the mission progresses, all that can be done at this time is to remind the reader that systematic errors of this sort could still be present in these data.

[7] http://archive.stsci.edu/kepler/release_notes/release_notes5/Data_Release_05_2010060414.pdf

3. POWER SPECTRAL DENSITY FUNCTIONS

3.1. *PSD Measurement*

The optical flux variations in AGN are aperiodic. A standard tool for characterizing such broadband (in temporal frequency) variability is the periodigram, which measures the fluctuation power spectral density (PSD) function. AGN PSDs have been best studied in the X-rays, where the PSDs show a broad shape that has been simply characterized as a double power law that breaks from a steep red noise high frequency slope of $\alpha_H \sim -2$ ($S \propto f^\alpha$, where α is the slope, S is the spectral density and f is the temporal frequency) to a flatter low frequency slope of $\alpha_L \sim -1$, at a break frequency f_b that typically corresponds to timescales of order a week, but scales with the mass of the black hole (e.g., Edelson & Nandra 1999, Uttley et al. 2002, Markowitz et al. 2003).

We used the Kepler SAP data to measure PSDs for all of these Kepler AGN. Currently, large photometric offsets introduced by quarterly spacecraft rolls prevent data from being combined across quarters, so these PSDs only cover individual quarters. This problem should eventually be solved, so we will produce PSDs covering longer timescales in a future paper.

For each light curve, a first order function was subtracted off so that the first and last points of the light curve were equal. This "end-matching" removes spurious low frequency power introduced by the cyclic nature of the PSD which tends to flatten the PSDs. (See Fougere 1985 for details.) This correction steepens the slopes by a mean value of 0.7, 0.3, 0.8 and 0.7 for Zw 229−15, KA 1925+50, KA 1858+48 and KA 1904+37, respectively. Fractional normalization was used, so the resulting power density has units of rms^2 Hz^{-1}.

The resulting PSDs (see Figure 3), fitted with a single power law ($S \propto f^\alpha$) plus noise model on temporal frequencies of $\sim 4 \times 10^{-7}$ to $\sim 4 \times 10^{-5}$ Hz (corresponding to timescales of ∼6 hours to ∼1 month), are very steep with slopes from $\alpha = -2.6$ to -3.3.

3.2. *Error analysis*

These PSDs also allow a check of the true noise level in the light curves. The fractional error, $err_{dir} = \langle err \rangle / \langle flux \rangle$, is reported in Column 4 of Table 2. An independent method of determining the error from the PSD uses the formula of Vaughan et al. (2003): $err_{ind} = \sqrt{\langle err^2 \rangle / \langle flux \rangle^2}$, and is given in Column 5. This reduces to the same quantity $\left(\langle err \rangle / \langle flux \rangle\right)$ in the limit of small fluctuations in the fluxes and errors, as is the case with these data. The errors derived from the PSD analysis are typically $\sim 25\%$ larger than the quoted light curve errors. This indicates the quoted errors are slightly underestimated, and that no other source of systematics dominates the quoted errors.

The PSD slopes for each quarter (listed in Table 2) show small scatter for individual objects. It is difficult to directly measure reliable errors on derived PSD slopes, but an estimate is provided by the observed dispersion for individual objects. For the two sources with the most data, Zw 229−15 and KA 1925+50, the mean slope and associated standard deviations are $\langle \alpha \rangle = -3.11 \pm 0.15$ and -2.67 ± 0.08. These differ by ∼2.5 standard deviations, suggesting, at very marginal significance, that the intrinsic difference between the derived slopes for these objects is larger than the associated errors.

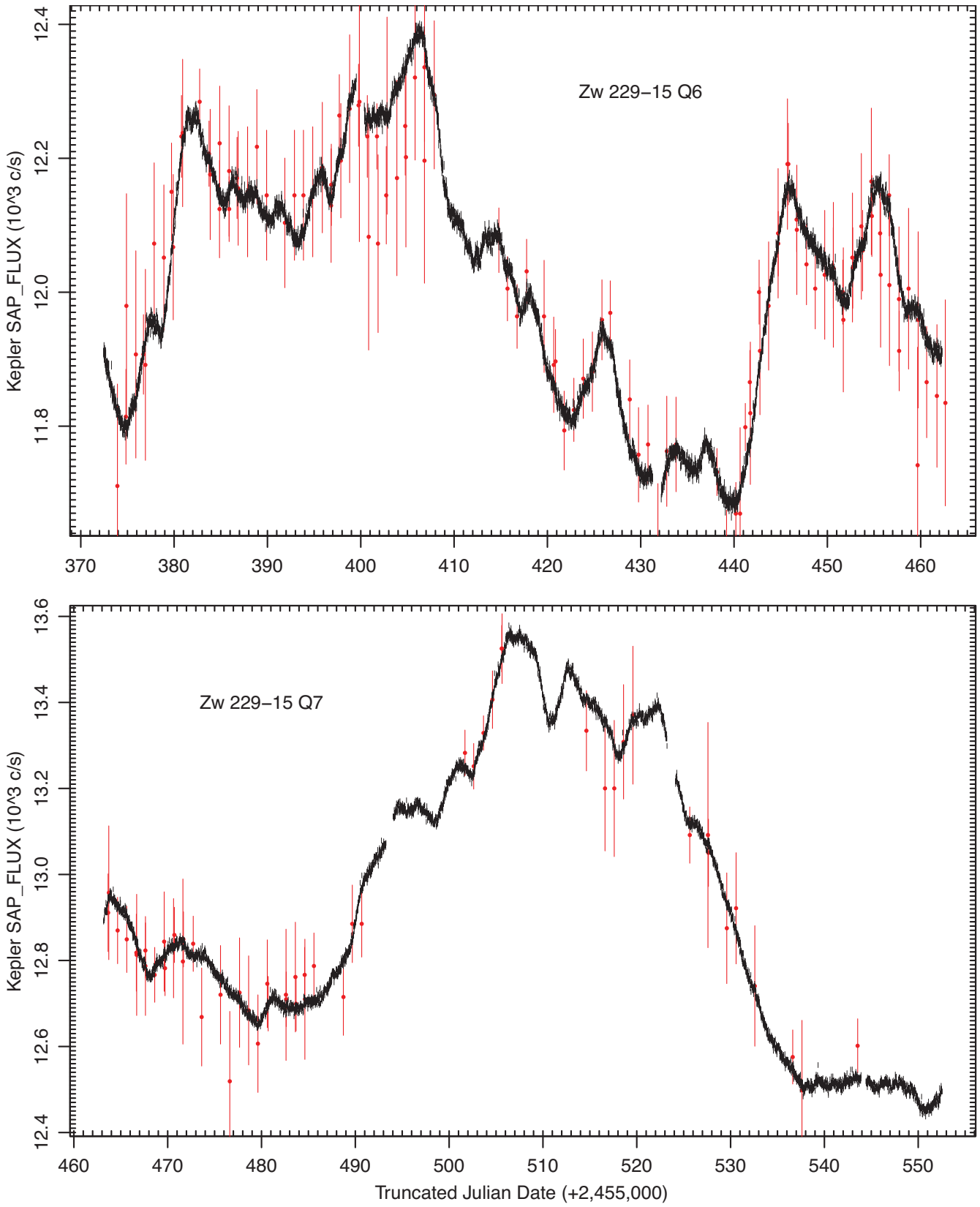

Figure 1. Kepler Q6 (top) and Q7 (bottom) light curves of the narrow line Seyfert 1 galaxy Zw 229−15 (in black). Each panel contains over 4,200 cadences, gathered one every ∼30 min, with a precision of $\lesssim$0.1%. A typical error bar is seen in the outlier at TJD ∼ 539. There are monthly ∼1 day data download gaps (e.g., TJD ∼ 431 and 524), but the overall duty cycle is > 90%. Note the ∼8% flux discontinuity between Q6 and Q7 as the quarterly spacecraft roll moves the source onto a different chip and a new SAP aperture is used. Note also the excellent agreement with simultaneous ground based LAMP data (shown in red; Barth et al. 2011), scaled to account for different aperture sizes.

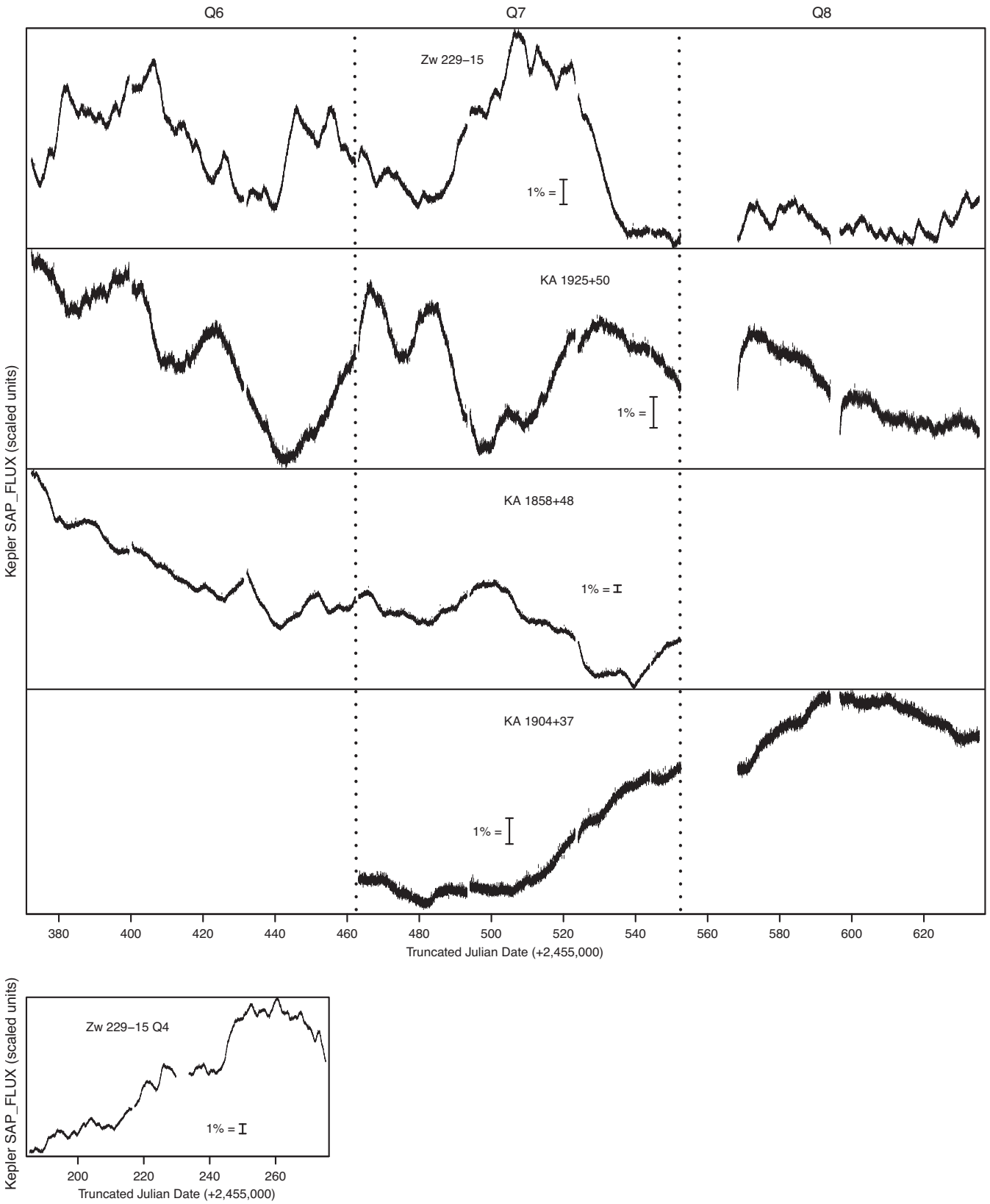

Figure 2. Q6–Q8 light curves for four variable Kepler AGN. A 1% bar is shown for scale. Q8 data were not obtained for KA 1858+48 because it fell on defective Module 3. Kepler observations of KA 1904+37 did not begin until Q7. Arbitrary offsets have been applied to match light curves across quarterly transitions (the dotted lines at TJD $\sim$ 462 and 552). Note the 16 day gap due to a safe mode event at the beginning of Q8; this makes the offset for that quarter highly uncertain. Note also that light curves occasionally show $\sim$1% discontinuities immediately following monthly data downloads or safe mode events (e.g., TJD $\sim$ 568 and 586 in KA 1925+50, and TJD $\sim$ 432 in Zw 229−15 and KA 1858+48) due to thermally induced focus changes.
The small bottom panel is the same as Figure 2a but for the Zw 229−15 Q4 data.

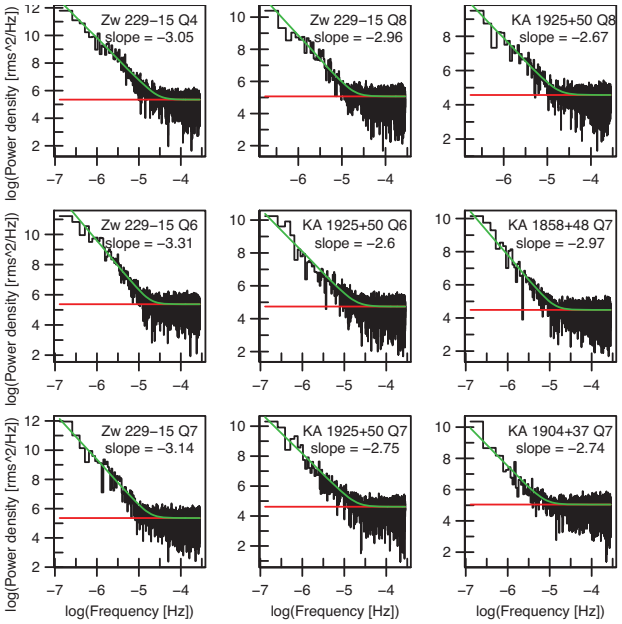

Figure 3. Optical PSDs and power law plus white noise fits for the 4 AGN in selected quarters over temporal frequencies $\sim 10^{-6.5}$ to $10^{-3.5}$ Hz. The fits are shown in green, and the noise level in red. Source name, quarter, and fitted power law slope (α) are given in the upper right of each plot.

Table 2
Kepler AGN Observations

Source Name	Quarter	10^3 cts s^{-1}	err_dir	err_ind	α
Zw 229–15	Q4	12.1	0.047%	0.065%	−3.05
Zw 229–15	Q6	12.0	0.051%	0.068%	−3.31
Zw 229–15	Q7	12.9	0.046%	0.062%	−3.14
Zw 229–15	Q8	10.4	0.052%	0.055%	−2.96
KA 1925+50	Q6	4.2	0.071%	0.084%	−2.60
KA 1925+50	Q7	3.8	0.065%	0.081%	−2.75
KA 1925+50	Q8	4.1	0.075%	0.078%	−2.67
KA 1858+48	Q6	2.1	0.117%	0.159%	−2.87
KA 1858+48	Q7	1.3	0.128%	0.207%	−2.97
KA 1904+37	Q7	5.8	0.071%	0.097%	−2.74
KA 1904+37	Q8	5.5	0.080%	0.087%	−2.95

Note. — Columns 1 and 2 give the source name and quarter, column 3 the mean `SAP_FLUX` count rate in units of 10^3 cts s^{-1}, and column 4 the ratio of the mean quoted errors divided by the mean flux. Column 5 gives the error rate derived from the PSD fits as discussed in Section 3.2. Column 6 gives the fitted PSD slopes (α) for each quarter.

(The quoted uncertainties are standard deviations of the distributions of the PSD slopes for different quarters.) Note that without the red noise leak correction, the standard deviations for these two sources would have been 0.58 and 0.22, respectively, so our correction successfully reproduces similar PSD slopes between the various quarters for each source. Since PSD analyses are notoriously susceptible to analytical systematics (see e.g., Vaughan et al. 2003) and there is the possibility that currently unknown systematic errors could affect these new Kepler data (see Sect. 2.2), the agreement in slope from quarter to quarter provides a degree of confidence that the observed steep slopes are accurate.

4. DISCUSSION

4.1. *Comparison to Previous Results*

4.1.1. *Optical Data*

Kepler light curves are of much higher quality and sampling rate than previous data. For example: in the data used by Kelley et al. (2009) the highest photometric quality is from the MACHO survey of Geha et al. (2003) which has ∼5% photometric errors and 600 good photometric measurements over 7.5 years, and thus samples at ∼1 point every 4.5 days compared to the 0.1% Kepler errors and 1 data point roughly every 30 minutes. Previous attempts to derive the PSD over a wide range of timescales have had to combine the data from many objects and several surveys (Hawkins 2002) or have relied on relatively sparsely sampled data, from several different telescopes (Breedt et al. 2010).

Previous results (e.g. Kelly et al 2009) tend to find best fitting PSDs with slopes of ~ -1.8 for the collective sample, rather flatter than what we have found. Since the Kepler PSDs cannot continue to very low frequencies with such steep slopes without implying very large variability amplitudes, there must be a break at timescales $>$ 1 month, which may make the Kepler PSDs consistent with previous work. It is not surprising that the results of our observations are rather different than what has been published previously—the other observations could not see the effects we are detecting. While there is a formal overlap in sampled timescales between our Kepler and other data, the much larger error bars for the previous PSDs (e.g. Breedt et al. 2010,) at characteristic frequencies above a few $\times 10^{-5}$ Hz makes comparison difficult. However, for at least one object, NGC 4051 (Breedt et al 2010), the observed PSD in the 10^{-6}– 10^{-8} Hz range is well determined and is flatter than our Kepler results for all of our objects. One possible explanation for the differences may lie in the different luminosities or Eddington ratios of the objects, since NGC 4051 is significantly less luminous and probably less massive than the objects in our sample.

4.1.2. *X-ray Data*

Although the particular Seyfert 1s in our sample do not have measured X-ray PSDs, many other Seyfert 1s have had X-ray PSDs measured over these timescales. These are always much flatter, typically having high frequency slopes of −1 to −2 (Edelson & Nandra 1999, Uttley et al. 2002, Markowitz et al. 2003). Thus our measurement of steep optical PSDs on short timescales is somewhat surprising because it is so different from that measured in the X-rays, and because Seyfert 1 optical and X-ray light curves appear to track well, at least on longer timescales (Uttley et al. 2003).

4.2. *Physical Implications for Accretion Disks*

The characteristic timescales of the fluctuations should correspond to different physical mechanisms which may be related to the size of the system, the dynamical timescales, epicyclic frequencies, g-modes or other characteristic timescales which could influence the source of variance. Since the source of the accreting material in AGN is not known, it is unclear if the sources of the perturbations are changes in the accretion flow, the turbulence due to physics in the disk itself (from the magnetorotational instability mechanism (MRI), e.g. Miller & Reynolds 2009, Noble & Krolik 2009), or perhaps other physics. As shown by McHardy et al. (2006), the characteristic timescale seen in the X-ray PSDs is related to the AGN mass and the accretion rate. However, it is not known if this is also true for the optical PSDs (MacLeod et al. 2010).

Recent results from ground based optical observations (e.g. Kelly et al. 2009, MacLeod et al. 2010) find that their results are consistent with a "damped random walk model". However, their light curves are irregularly and more sparsely sampled compared to Kepler data (see Figure 2 in Kozlowski et al. 2010). Our data do not find the predicted f^{-2} power spectrum at high frequencies predicted by this model. However, since there is very little overlap in frequencies and our sample size is much smaller, direct comparison is difficult. Our data are just capable of reaching the light travel time size of the disks on our sampled AGN. The effective size of the region emitting radiation at a given frequency is (Baganoff & Malkan 1995):

$$r_{1/2} = 7.5 \times 10^{23} \epsilon^{-1/3} \nu^{-4/3} (\mathrm{M/M_\odot})^{-1/3} (\mathrm{L/L_{Edd}})^{1/3} r_G,$$

where r_G is the Schwarzschild radius, ϵ is the accretion efficiency and ν is the effective observing frequency of the data. Utilizing an effective wavelength of 5000Å, mass of 1×10^7 $M_\odot$ (Barth et al 2011) and Eddington ratio of 0.05 we find an effective light travel time ($r_{1/2}/c$) of $\sim$1 day which is close to our white noise limit of 0.25 days. The 4 sources in this paper span only 1 order of magnitude in X-ray luminosity ($\log L_X = 42.6$ to 43.6) and thus, probably, a small range in mass. Our future observations we will have a larger number as well as more luminous objects and thus we should constrain the limits where light travel time effects can be well measured.

While modeling of accretion disks from first principles via magnetohydrodynamic (MHD) calculations is in its early days there are several estimates of the slope of the PSD from accretion disks. In these models the underlying physical drivers for variability in the light curve are variations in the accretion rate caused by the chaotic character of MHD turbulence. Noble and Krolik (2009) simulate emission from the coronae appropriate to the X-ray emission, and thus it is not clear if their simulation is comparable with our results. Chan et al. (2009) focus on Sgr A* which seems to be accreting in a different mode than the Seyfert 1s in our sample. Reynolds & Miller (2009) show PSDs of the mass accretion rate whose high frequency slopes (~ -2.9) are very close to those seen in our observations. However, their simulation was only run for a relatively short time ($\sim 1.2 \times 10^4\ GM/c^3$) which corresponds to 14 days for objects of the mass of Zw 229−15.

All simulations so far suffer from the fundamental problem that to compare them with observations one has to convert the simulated disk characteristics into a radiation flux spectrum. Thus it is not clear that the proxies for emission developed so far are appropriate. This problem is fully recognized by the simulators and thus, in general, they have been loath to directly compare to the data.

5. CONCLUSIONS

Power spectral analysis of four AGN observed by Kepler during Q6-Q8 show very steep ($\alpha \sim -2.6$ to -3.3) slopes, considerably steeper than that seen in the X-rays. The PSDs for each source are consistent from quarter to quarter and, at $> 2\sigma$ confidence, are different from each other. Analysis of these high quality light curves indicates that the influence of systematic errors is rather small; additionally, direct comparison of Kepler and LAMP monitoring of Zw 229−15 shows excellent agreement. Comparison with analytic models of AGN variability shows steeper than predicted slopes; however, comparison with MHD simulations seems to show better agreement. Further analysis of other characteristics of the light curve, longer time series, the analysis of more objects and the comparison to semi-analytic models of time variability will be the subject of future papers. We hope that these new high quality Kepler data will stimulate the calculation of the time series from accretion disks.

We thank the Kepler team for their efforts to make the data accessible and tractable and the Kepler GO program for funding, Matt Malkan for extensive contributions to the identification of new Kepler AGN, Simon Vaughan for valuable help with PSD measurements and Aaron Barth and the LAMP team for early access to their data.

REFERENCES

Arévalo, P., Uttley, P., Lira, P., et al. 2009, MNRAS, 397, 2004
Baganoff, F. K., & Malkan, M. A. 1995, ApJ, 444, L13
Barth, A. J., Nguyen, M. L., Malkan, M. A., et al. 2011, ApJ, 732, 121
Borucki, W. J., Koch, D., Basri, G., et al. 2010, Science, 327, 977
Breedt, E., Arévalo, P., McHardy, I. M., et al. 2009, MNRAS, 394, 427
Chan, C.-k., Liu, S., Fryer, C. L., et al. 2009, ApJ, 701, 521
Edelson, R., Turner, T. J., Pounds, K., et al. 2002, ApJ, 568, 610
Edelson, R., Malkan, M. 2011, AJ, in preparation
Edelson, R., & Nandra, K. 1999, ApJ, 514, 682
Falco, E. E., Kurtz, M. J., Geller, M. J., et al. 1999, PASP, 111, 438
Fougere, P. F. 1985, J. Geophys. Res., 90, 4355
Frank, J., King, A., & Raine, D. J. 2002, Accretion Power in Astrophysics. Cambridge, UK: Cambridge University Press
Geha, M., Alcock, C., Allsman, R. A., et al. 2003, AJ, 125, 1
Hawkins, M. R. S. 2002, MNRAS, 329, 76
Jenkins, J. M. et al. 2010, ApJ, 713, L87
Kelly, B. C., Bechtold, J., & Siemiginowska, A. 2009, ApJ, 698, 895
Kochanek, C. S. 2004, ApJ, 605, 58
Kozłowski, S.,Kochanek, C. S., Udalski, A., et al. 2010, ApJ, 708, 927
MacLeod, C. L., Ivezić, Ž., Kochanek, C. S., et al. 2010, ApJ, 721, 1014
Malkan, M. 2004, AGN Physics with the Sloan Digital Sky Survey, 311, 449
Markowitz, A., Edelson, R., Vaughan, S., et al. 2003, ApJ, 593, 96
McHardy, I. M., Koerding, E., Knigge, C., Uttley, P., & Fender, R. P. 2006, Nature, 444, 730
McHardy, I. M., Arévalo, P., Uttley, P., et al. 2007, MNRAS, 382, 985
Reynolds, C. S., & Miller, M. C. 2009, ApJ, 692, 869
Moran, E. C., Helfand, D. J., Becker, R. H., & White, R. L. 1996, ApJ, 461, 127
Noble, S. C., & Krolik, J. H. 2009, ApJ, 703, 964
Proust, D. 1990, IAU Circ., 5134, 2
Quintana, E. V., Jenkins, J. M., Clarke, B. D., et al. 2010, Proc. SPIE, 7740,
Shakura, N. I., & Sunyaev, R. A. 1973, A&A, 24, 337
Stocke, J. T., Liebert, J., Gioia, I. M., et al. 1983, ApJ, 273, 458
Skrutskie, M. F., Cutri, R. M., Stiening, R., et al. 2006, AJ, 131, 1163
Timmer, J., & Koenig, M. 1995, A&A, 300, 707
Twicken, J. D., Clarke, B. D., Bryson, S. T., et al. 2010, Proc. SPIE, 7740,
Uttley, P., McHardy, I. M., & Papadakis, I. E. 2002, MNRAS, 332, 231
Uttley, P., Edelson, R., McHardy, I. M., Peterson, B. M., & Markowitz, A. 2003, ApJ, 584, L53
Vaughan, S., Edelson, R., Warwick, R. S., & Uttley, P. 2003, MNRAS, 345, 1271
Voges, W., Aschenbach, B., Boller, T., et al. 1999, A&A, 349, 389